ceramics

MDPI

Article

Thermal Mechanical Property Enhancement with Silicon Carbide Ceramic Filled Composites for Industrial Applications

Kalinga Hapuhinna [1], Rajitha D. Gunaratne [1,*] and Jagath Pitawala [2]

[1] Department of Materials and Mechanical Technology, Faculty of Technology, University of Sri Jayewardenepura, Homagama 10200, Sri Lanka
[2] Department of Science & Technology, Faculty of Applied Sciences, Uva Wellassa University, Badulla 90000, Sri Lanka
* Correspondence: rajitha@sjp.ac.lk

Abstract: Epoxy composites with glass fiber reinforcement can be found in the automotive and aerospace industries. In this study, the properties of the epoxy matrix were enhanced by processing composites filled with ceramic particles of silicon carbide (SiC). At first, SiC-filled E-glass fiber-reinforced epoxy composites/sandwich structures were processed using the hand layup technique. Next, processed composites were characterized using a tensile tester and an Izod impact tester to determine the best mixing ratio of ceramic-embedded epoxy composites. The highest mechanical properties were obtained according to ASTM D638 and D256 standards. Next, Fourier transform infrared spectroscopy (FTIR), scanning electron microscopy (SEM), x-ray diffraction analysis (XRD), analysis of differential scanning calorimetry (DSC), and thermogravimetric analysis (TGA) were carried out respectively to find out the presence of functional groups, surface morphology, crystallographic structure, glass transition temperature (Tg) and thermal/material stability of processed composites. In the end, the study elaborates that the mechanical properties of epoxy matrix composites were improved by the addition of SiC ceramic fillers, and among processed composites, 10%SiCE composite carried the highest properties, including the Tg value of 62.8 °C, 69.87 MPa for tensile strength and 57.12 kJ m^{-1} for impact strength.

Keywords: silicon carbide; ceramic fillers; composites; thermal properties; mechanical properties; industrial applications

Citation: Hapuhinna, K.; Gunaratne, R.D.; Pitawala, J. Thermal Mechanical Property Enhancement with Silicon Carbide Ceramic Filled Composites for Industrial Applications. *Ceramics* **2022**, *5*, 721–730. https://doi.org/10.3390/ceramics5040052

Academic Editor: Adel Mohamed Amer Mohamed

Received: 6 September 2022
Accepted: 11 October 2022
Published: 13 October 2022

1. Introduction

The thermal and mechanical properties of a composite affect the range of efficacy of the material and the expected service life. Most structural materials are triclinic, which means their mechanical properties change depending on their orientation. The change in properties can be attributed to changes in the microstructure of the fiber/filler and matrix reinforcement [1–7].

Many different loading scenarios can be applied to the materials, and the composite performance is dependent on the loading conditions. It is also needed to ascertain the effect of temperature change on the properties of fiber-reinforced epoxy composites because an increase in temperature results in a decrease in strength and ductility, whereas a decrease in temperature leads to an improvement in ductility and strength.

Aside from fiber-reinforced polymer composites, composites with both fiber and filler reinforcement performed well in a variety of practical situations. Due to trade embargos, we couldn't purchase cost carbon fiber in our country. To rater the higher needs of the structural properties, we have designed these composites with SiC embedded epoxy glass fiber composite as SiC and glass fiber are more compatible, resulting in advanced composite with higher mechanical properties.

To improve the mechanical properties of fiber-reinforced epoxy, silicon carbide (SiC) filler particles [8–14] were added. The influence of particle size, shape, and percentage content on the mechanical properties of fiber-reinforced polymer composites is a major topic. According to research, the configuration and form of silica particles have a significant impact on mechanical properties such as impact resistance, tensile strength, and fracture properties.

The preceding literature provides a brief overview of the effects of fiber/filler addition on the mechanical and thermal properties of SiC-filled glass fiber-reinforced epoxy composites [15–20]. The addition of fiber/filler reinforcement to matrix composites has been shown to determine various mechanical properties at optimum fiber loading conditions [21–24]. Due to its distinctive combination of properties, including excellent oxidation resistance, strength retention at high temperatures, high fatigue strength, high thermal conductivity, and better thermal shock resistance, SiC has gained recognition as a significant structural ceramic material. There are several methods that can be used to synthesize SiC material, such as laser ablation, sol-gel, vapor-solid, chemical vapor deposition (CVD) and vapor-liquid-solid methods [25–29]. Both micro/nano range SiC ceramics were used in previous studies. The extremely covalent (up to 88%) chemical interaction between silicon and carbon atoms is what causes such a combination of characteristics. The polytypism of silicon carbide, or the production of a wide variety of distinct structural changes without any change in composition, is the material's most noticeable characteristic of SiC. Considering the variety of properties, SiC can be applied in various applications in various fields such as biomedical engineering, automotive, aerospace and other industrial applications like luminescent, nuclear technologies etc. [30–34].

The current study aimed to find out the applicability of newly processed silicon carbide ceramic-filled E-glass fiber-reinforced epoxy composites for industrial applications with the enhancement of thermal and mechanical properties.

2. Materials and Methods

2.1. Materials

The main raw materials for this study were cubic silicon carbide (SiC), −200 mesh particle size (Sigma Aldrich, Saint Louis, MO, USA), commercially available epoxy resin and hardener (Fast Fix-FX E400, Taiwan), and silane-treated E-glass fiber chopped strand mats of 450g/m^2.

2.2. Methods

2.2.1. Composite Preparation

As indicated in Figures 1 and 2, at first, the study processed cross-linked pure epoxy matrix (0%NE) material without the addition of silicon carbide (SiC) as the "control." Next, a series of silicon carbide embedded E-glass fiber reinforced epoxy matrix composites (SiCE composites) were processed as bellows; masses of the SiC ceramic filler were calculated according to the required weight fractions (0, 5, 10, 15, 20, 25, 30, 35, 40, 45, 50, 55, 60, 65, 70, 75, 80, 85, 90) wt% of the epoxy mixture (mixture of epoxy resin and hardener). It was well mixed separately for 10 min at room temperature continuously and slowly to avoid bubbling during mixing. (Considering epoxy's gelation and curing time according to 25 °C room temperature.) After that, the mixture was uniformly poured from one corner into the molds until the required filling level (to avoid bubbles formation, which may lead to cast damage) with the addition of 10 fiber mats into the sample to buildup sandwich-structures as shown in Figure 3. Finally, the mixtures were left in the molds for 24 h at room temperature to solidify.

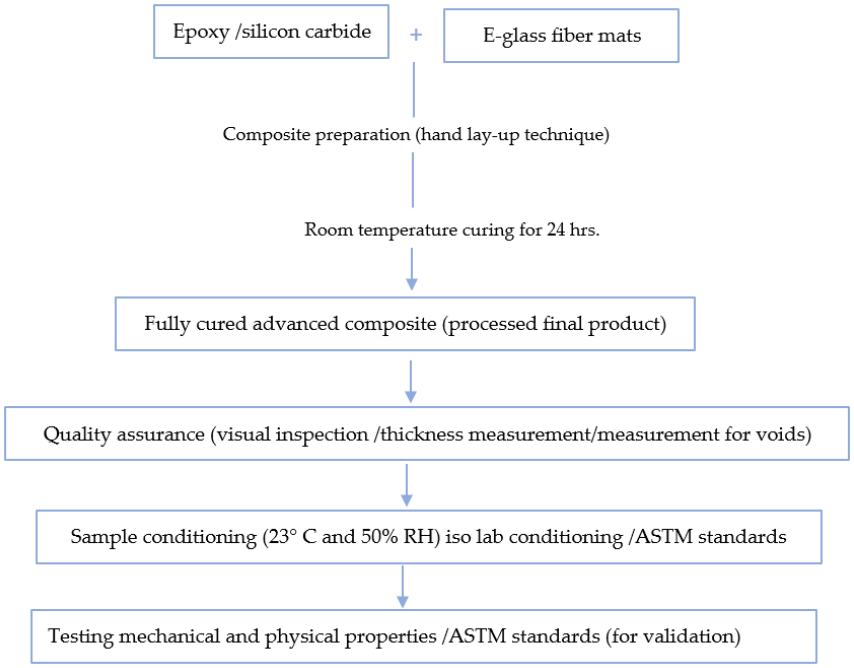

Figure 1. Flow chart for composite preparation & characterization.

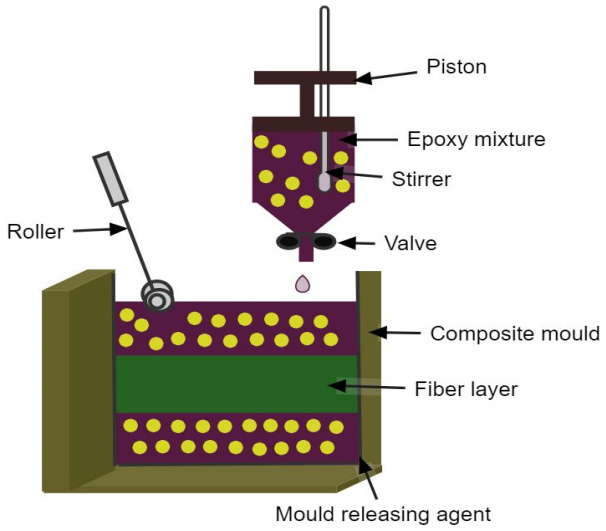

Figure 2. The schematic diagram for processing SiC ceramic embedded E-glass fiber reinforced epoxy matrix composites using hand layup technique.

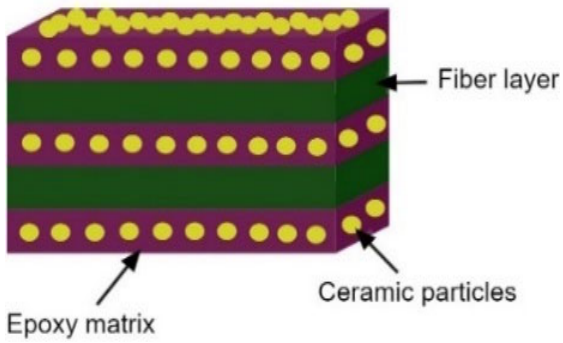

Figure 3. The sandwich-structure of processed SiC ceramic embedded E-glass fiber reinforced epoxy matrix composites.

2.2.2. Composite Characterization

All processed composites, including control, were characterized under a hydraulic universal testing machine (HLC-100) and an Izod impact tester (HEXA PLAST) to determine the best mixing ratio of filler and the epoxy matrix having the highest tensile and impact properties. All the tests were conducted according to ASTM D638 and D256 standards. The following characterization techniques were performed for the control and the sample with the highest mechanical properties: FTIR spectroscopy (Bruker-Alpha, Bruker, Billerica, MA, USA) across the range (400 cm^{-1}–4000 cm^{-1}); 4 cm^{-1} resolution was used to determine the composition, primarily the presence of functional groups. SEM with EDS analysis (Hitachi SU6600, Hitachi, Tokyo, Japan) was conducted to examine the elementary composition, presence of impurities, and surface morphology of micro/nanostructural features. XRD analysis ((Rigaku-Ultima. IV diffractometer) was carried out in reflection mode with CuK1: 0.154 nm radiation, 1.5° min^{-1} scanning speed within the (15°–80°) ranged angles as two values to determine their crystallographic phases. DSC analysis was done using a differential scanning calorimeter (TA-Q200) under an N environment, 100°C min^{-1} heating rate, up to 650 °C maximum temperature, to find out the variation of glass transition temperatures (Tg values). Finally, thermogravimetric analysis (TA-SDTQ600) was done using a thermal analyzer under an N environment, 20 °C min^{-1} heating rate, up to a maximum temperature of 1400 °C, to find out the thermal stability.

3. Results & Discussion

3.1. Results of SEM Analysis

The flow of epoxy and the impregnation of glass fibers were depicted in Figure 4 to Figure 5 SEM micrographs. According to the findings, the resin was evenly distributed across the fabric, and the adhesive interaction of the epoxy matrix, SiC ceramic filler, and E-glass fiber was flawless. The apparent epoxy matrix adhesion of the matrix is deciphered, and ceramic filler glass fibers are inserted. All phases of materials appear to have superior interfacial bonding. SEM images were also interpreted as brittle fractures in composite materials.

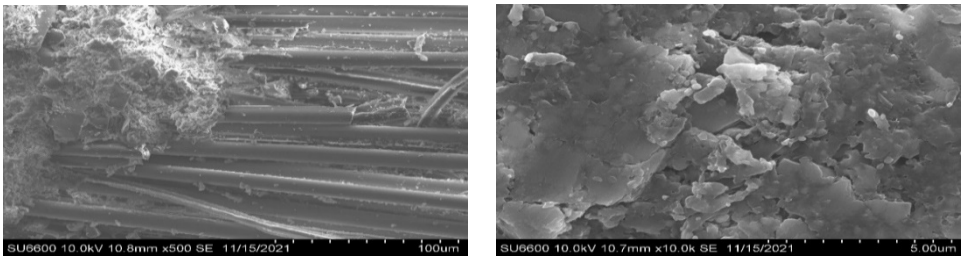

(**a**) (**b**)

Figure 4. SEM images for NE (control) at 10kV with magnifications (**a**) 500 (**b**)10000.

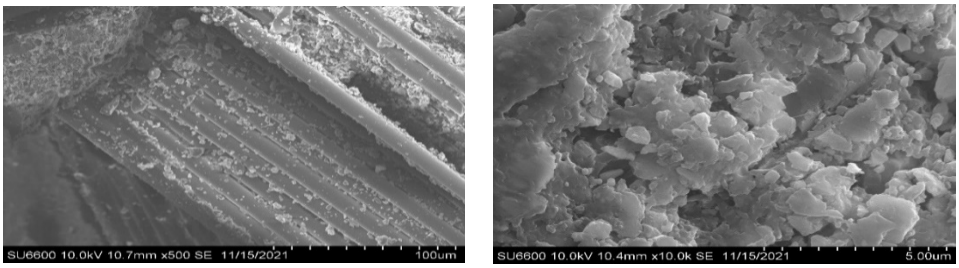

(**a**) (**b**)

Figure 5. SEM images for 10%SiCE at 10kV with magnifications (**a**) 500 (**b**)10000

3.2. Results of FTIR Analysis

According to Figure 6, it can be stated that all the processed composites and the control carry peaks related to the epoxy matrix and E-glass fiber reinforcement. The bands observed at 918 cm^{-1}, 1675 cm^{-1}, and 2925 cm^{-1} are assigned to the vibrations of the epoxy ring, aldehyde groups, and aromatic protons in the epoxy matrix, respectively. The bands observed at the 3200 cm^{-1}, 3135 cm^{-1}, 1800 cm^{-1}, and 1122 cm^{-1}, corresponding to –NH/OH, $–CH_2$, and $–C_2H_5$, $–NH_2$, Si-O-Si vibrational modes in E-glass fiber reinforcement. The –OH band centered at about 3500 cm^{-1} in both curves corresponds to the absorbed water molecules. Apart from those peaks, when considering the 10%SiCE composite, it exhibited characteristic peaks of nearly 812 cm^{-1}, 813 cm^{-1}, 917 cm^{-1}, 972 cm^{-1}, 1018 cm^{-1}, 1082 cm^{-1}, 1258 cm^{-1} for vibrational modes of SiC [35–38].

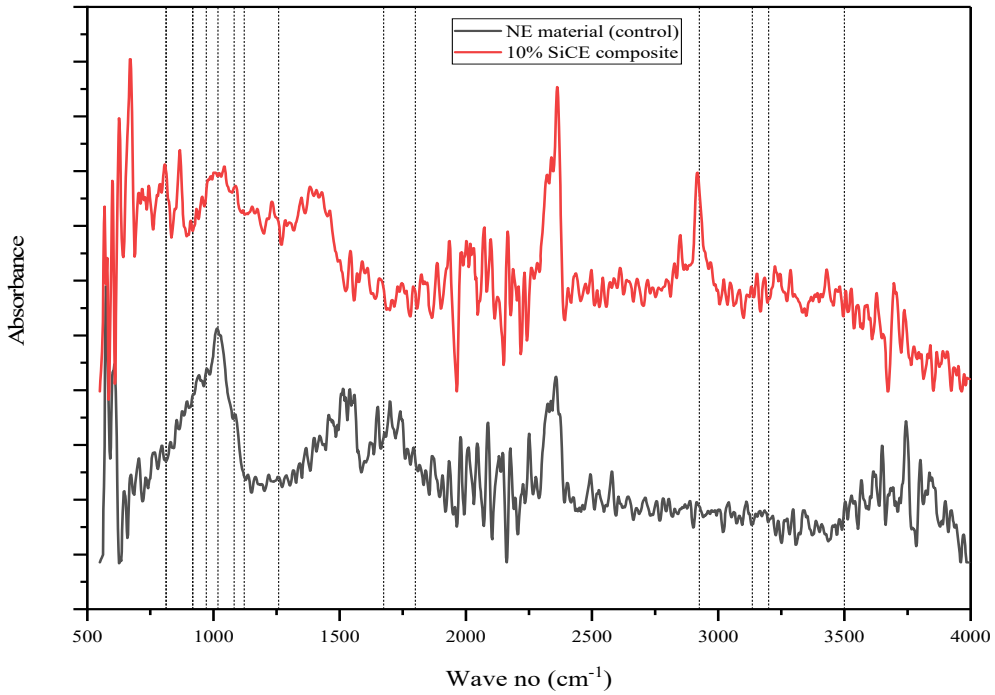

Figure 6. The resulting FTIR spectrum of processed epoxy matrix composites.

3.3. Results of XRD Analysis

As shown in Figure 7, crystalline characteristics can be found in all processed ceramic-incorporated glass fiber-reinforced epoxy composites and pure cross-linked epoxy material (control). All the peaks associated with the SiC filler are present in the respective composite samples, their peak intensity is very low, and epoxy peaks are the prominent peaks. Peaks associated with the epoxy matrix were found within the NE material (control sample). Apart from those peaks, all the other peaks related to the crystallographic phases of cubic silicon carbide, including (111), (220), and (311), are present in the XRD diffractogram of the 10%SiCE composite. Apart from those, Figure 8 describes that E glass fiber mat carried amorphous properties [39,40].

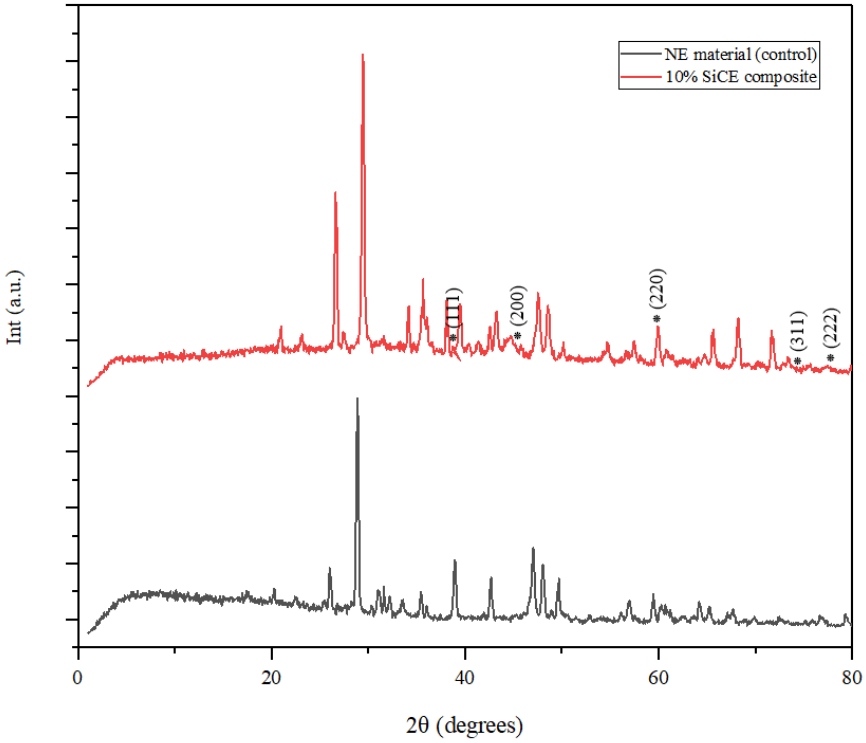

Figure 7. XRD diffractogram of the processed control and the 10%SiCE composite samples.

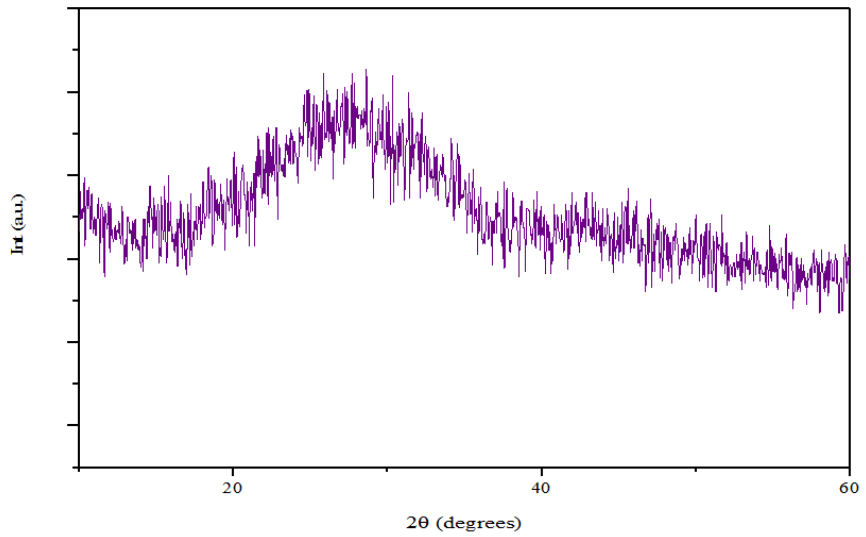

Figure 8. XRD diffractogram of E-glass fiber mat.

3.4. Results of Tensile Tests

The results in Table 1 clearly interpreted that; the highest tensile strength values for processed SiCE composite series are 69.87 MPa for 10%SiCE composite. When comparing those results with the pure NE material, tensile strength has increased nearly four times. The addition of SiC ceramic fillers into the fiber-reinforced epoxy matrix composites increased the interfacial bonding strength between fibers, epoxy and fillers, leading to greater tensile values. Brittle fractures were found in all of the processed composites.

Table 1. Results of tensile tests for all processed epoxy matrix composites

Processed Composites		Impact Strength (kJ m^{-1})	
		Avg Value	**SD Value**
Control	0%NE	16.22	0.22
SiCE composites	5%SiCE	58.43	0.74
	10%SiCE	69.87	0.67
	15%SiCE	66.29	0.67
	20%SiCE	55.72	0.67
	25%SiCE	51.38	1.11
	30%SiCE	52.25	0.43
	35%SiCE	23.43	0.21
	40%SiCE	38.12	1.12
	45%SiCE	34.82	0.54
	50%SiCE	31.17	0.72
	55%SiCE	23.83	1.56
	60%SiCE	11.92	0.37
	65%SiCE	11.30	0.71
	70%SiCE	10.72	0.42

Avg value—average value; SD value—standard deviation value. *** 70%, 75%, 80%, 85%, 90% and 95% hydroxyapatite filler added epoxy composites are too much brittle

3.5. Results of DSC Analysis

Variation of Tg values for the processed composites samples with maximum tensile properties and the control mentioned in Table 2. Those results showed that with the addition of the ceramic filler into the epoxy matrix with glass fiber reinforcement, glass transition temperatures were increased, which may occur as interactions between filler particles and the epoxy matrix intensify, reducing molecular mobility and flexibility of the polymer chains in the vicinity of the interfaces. Therefore, the overall curing of the epoxy composite was improved by adding SiC ceramic filler. On the other hand, the addition of SiC results in the reduction of free volume, higher heat absorption and higher heat conductivity which may also help to improve the cross-link density.

Table 2. Results of DSC analysis for all processed ceramic incorporated E-glass fiber reinforced epoxy composites.

Processed Composite	Glass Transition Temperature Tg (°C)
0% NE material (Control)	60.8
10%SiCE composite	62.8

3.6. Results of Impact Tests

As shown in Table 3, the highest impact strength values for processed SiCE composite series are 57.12 kJ m^{-1} for 10%SiCE composite, respectively. When comparing results for those three processed composite series, the addition of SiC ceramic fillers into the E-glass fiber-reinforced epoxy matrix composites can be given the highest impact values, similar to the tensile results.

Table 3. Results of impact tests for all processed ceramic incorporated E-glass fiber reinforced epoxy composites.

Processed Composites		Impact Strength (kJ m^{-1})	
		Avg Value	**SD Value**
Control	0%NE	53.37	0.15
SiCE composites	5%SiCE	56.81	0.12

	10%SiCE	57.12	0.15
	15%SiCE	57.08	0.15
	20%SiCE	57.03	0.06

Avg value—average value; SD value—standard deviation value

3.7. Results of TGA Analysis

Figure 9 shows a similar weight loss pattern in both TGA curves. It can be stated that the degradation of the samples occurred in three stages. The 1st stage may occur due to the weight loss accompanied by the endo effect indicating moisture removal from the samples up to 200 °C. Then the 2nd stage may occur between 250–350 °C, with the oxidation of carbon or with the removal of carbon dioxide gas from compounds. 3rd stage may occur due to the removal of remaining volatile compounds or the weight loss due to phase transformation from 400 °C up to 800 °C. When comparing and contrasting both curves, it can be seen that the addition of SiC ceramic fillers into the epoxy matrix led to increased mass loss. That may result in the effect of thermal degradation of SiC ceramic particles.

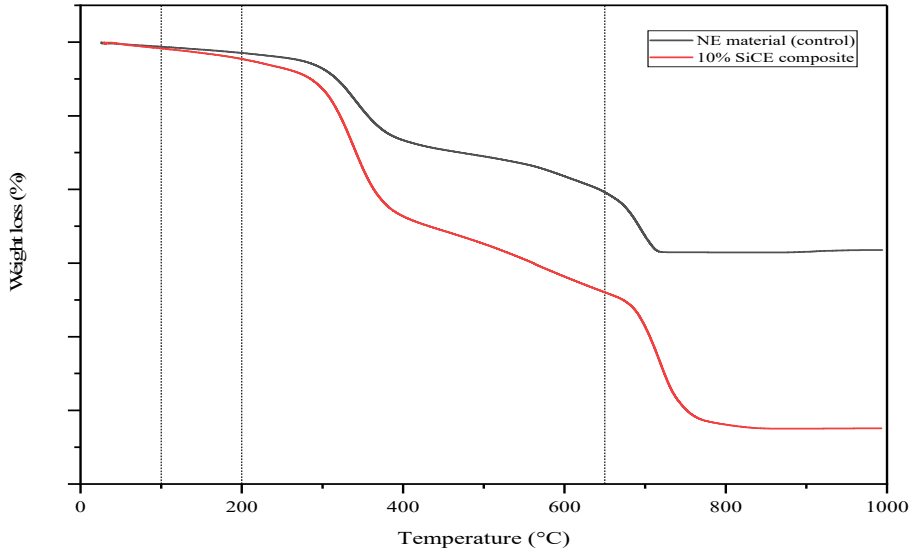

Figure 9. TGA analysis results of the processed epoxy matrix composites

4. Conclusions

It has been confirmed that the inherited qualities of epoxy ceramic fiber composites were significantly improved by adding SiC ceramic filler. Mechanical properties were drastically improved by adding SiC ceramic which is shown by the tensile results (10% is the highest), and a slight increase in thermal properties was observed in the TGA results.

In the beginning, tensile strength for NE material (control) was exhibited as 16.22 MPa, and the value for 10%SiCE composite was nearly 69.87 MPa. When comparing those results, it was shown that, with the addition of ceramic filler, tensile strength increased by four times. The impact strength of the NE material (control) was 53.37 kJ $m^{-1,}$ and the value for the 10%SiCE composite increased up to 57.12 kJ m^{-1}.

SEM micrographs of 10%SiCE fracture surfaces showed the continuous dispersal of SiC ceramic without any severe agglomerations. Extra ceramic addition beyond 70% enhances brittleness.

Among all processed composites, 10%SiCE composite demonstrated the most outstanding Tg value of 62.8 °C utilizing higher mechanical properties.

The addition of SiC ceramic filler into the epoxy matrix decreased free volume and increased cross-link density which leads to higher mechanical properties.

Processed ceramic filler-added epoxy matrix composites could also be used for aeronautical, appliance, architecture, automotive, construction, energy, marine, corrosive and environmental applications.

Author Contributions: Conceptualization, K.H., R.D.G. and J.P.; methodology, K.H., R.D.G. and J.P.; investigation, K.H., R.D.G. and J.P.; writing—original draft preparation, K.H..; writing—review and editing, K.H., R.D.G. and J.P.; supervision, R.D.G. and J.P.; funding acquisition, R.D.G. All authors have read and agreed to the published version of the manuscript.

Funding: This research was fully funded by the university research grants, UNIVERSITY OF SRI JAYEWARDENEPURA, SRI LANKA, grant number ASP/01/RE/FOT/2019/61.

Institutional Review Board Statement: Not applicable.

Informed Consent Statement: Not applicable.

Data Availability Statement: Data available in the paper.

Acknowledgments: We would like to acknowledge M.D. Nilantha, G.M.M.S. Duminda, R.M.N.B. Bandara, R. Jawahir, R.R. De Silva, A.C.P. Aththaragama technical officers, and P.H.G.P.N. Ranathunga, and P.S.S. Bandara lab assistants of Uva Wellassa University for their technical support throughout this study.

Conflicts of Interest: The authors declare no conflict of interest.

References

1. Latha, P.S.; Rao, M.V. Investigation into Effect of Ceramic Fillers on Mechanical and Tribological Properties of Bamboo-Glass Hybrid Fiber Reinforced Polymer Composites. *Silicon* **2018**, *10*, 1543–1550.
2. Scaffaro, R.; Di Bartolo, A.; Dintcheva, N.T. Matrix and filler recycling of carbon and glass fiber-reinforced polymer composites: A review. *Polymers* **2021**, *13*, 3817.
3. Ahmed, K.S.; Mallinatha, V.; Amith, S.J. Effect of ceramic fillers on mechanical properties of woven jute fabric reinforced epoxy composites. *J. Reinf. Plast. Compos*. **2011**, *30*, 1315–1326.
4. Raja, R.S.; Manisekar, K.; Manikandan, V. Effect of fly ash filler size on mechanical properties of polymer matrix composites. *Int. J. Mining Metall. Mech. Eng*. **2013**, *1*, 34–38.
5. Ashok, K.G.; Kalaichelvan, K.; Damodaran, A. Effect of Nano Fillers on Mechanical Properties of Luffa Fiber Epoxy Composites. *J. Nat. Fibers*. **2022**, *19*, 1472–1489. https://doi.org/10.1080/15440478.2020.1779898.
6. Liu, J.; Yan, H.; Jiang, K. Mechanical properties of graphene platelet-reinforced alumina ceramic composites. *Ceram. Int.* **2013**, *39*, 6215–6221. https://doi.org/10.1016/j.ceramint.2013.01.041.
7. Hemanth, R.; Sekar, M.; Suresha, B. Effects of Fibers and Fillers on Mechanical Properties of Thermoplastic Composites. *Indian J. Adv. Chem. Sci.* **2014**, *2*, 28–35.
8. Liu, G.; Zhang, X.; Yang, J.; Qiao, G. Recent advances in joining of SiC-based materials (monolithic SiC and SiCf/SiC composites): Joining processes, joint strength, and interfacial behavior. *J. Adv. Ceram.* **2019**, *8*, 19–38.
9. Yao, Y.; Huang, F.; Bai, X.; Zeng, X.; Xu, J.-B.; Sun, R.; Deng, F.; Xin, P. Facile Fabrication of Silicon Carbide Spheres and Its Application in Polymer Composites with Enhanced Thermal Conductivity. In Proceedings of the 2020 21st International Conference on Electronic Packaging Technology (ICEPT), Guangzhou, China, 12–15 August 2020.
10. Yang, Y.; Pössel, B.; Mülhaupt, R. Graphenated Ceramic Particles as Functional Fillers for Nonisocyanate Polyhydroxyurethane Composites. *Macromol. Mater. Eng*. **2020**, *305*, 2000203.
11. Zhang, K.; Zhang, L.; He, R.; Wang, K.; Wei, K.; Zhang, B. Joining of Cf/SiC Ceramic Matrix Composites: A Review. *Adv. Mater. Sci. Eng*. **2018**, *2018*, 6176054.
12. Davis, R.F. Silicon Carbide. *Ref. Modul. Mater. Sci. Mater. Eng*. **2017**, 1–10. https://doi.org/10.1016/B978-0-12-803581-8.02445-0
13. Smith, T.P.; Davis, R.F. Silicon Carbide. *Encycl. Mater. Sci. Technol.* **2001**, 1–6. https://doi.org/10.1016/B0-08-043152-6/01518-7
14. Locke, C.W.; Severino, A.; La Via, F.; Reyes, M.; Register, J.; Saddow, S.E. SiC Films and Coatings: Amorphous, Polycrystalline, and Single Crystal Forms. In *Silicon Carbide Biotechnology*, 1st ed.; Elsevier: Amsterdam, The Netherlands, 2012; pp. 17–61. https://doi.org/10.1016/B978-0-12-385906-8.00002-7.
15. Kiran, M.D.; Govindaraju, H.K.; Jayaraju, T. Evaluation of Mechanical Properties of Glass Fiber Reinforced Epoxy Polymer Composites with Alumina, Titanium dioxide and Silicon Carbide. *Mater. Today Proc*. **2018**, *5*, 22355–22361. https://doi.org/10.1016/j.matpr.2018.06.602.
16. Agarwal, G.; Patnaik, A.; Sharma, R.K. Thermo-mechanical properties of silicon carbide filled chopped glass fiber reinforced epoxy composites. *Int. J. Adv. Struct. Eng*. **2013**, *5*, 21.
17. Agarwal, G.; Patnaik, A.; Sharma, R.K. Thermo-Mechanical Properties and Abrasive Wear Behavior of Silicon Carbide Filled Woven Glass Fiber Composites. *Silicon* **2014**, *6*, 155–168.

18. Vaggar, G.B.; Kamate, S.C.; Badyankal, P.V. A study on thermal conductivity enhancement of silicon carbide filler glass fiber epoxy resin hybrid composites. *Mater. Today Proc*. **2019**, *35*, 330–334. https://doi.org/10.1016/j.matpr.2020.02.008.
19. Arpitha, G.R.; Sanjay, M.R.; Naik, L.L.; Yogesha, B. Mechanical Properties of Epoxy Based Hybrid Composites Reinforced with Sisal/SIC/Glass Fibers. *Int. J. Eng. Res. Generic Sci.* **2014**, *2*, 398–405.
20. Antil, P. Modelling and Multi-Objective Optimization during ECDM of Silicon Carbide Reinforced Epoxy Composites. *Silicon* **2020**, *12*, 275–288.
21. Biswas, S. Mechanical properties of bamboo-epoxy composites a structural application. *Adv. Mater. Res.* **2012**, *1*, 221–231.
22. Nayak, R.K.; Dash, A.; Ray, B.C. Effect of Epoxy Modifiers (Al_2O_3/SiO_2/TiO_2) on Mechanical Performance of epoxy/glass Fiber Hybrid Composites. *Procedia. Mater. Sci*. **2014**, *6*, 1359–1364. https://doi.org/10.1016/j.mspro.2014.07.115.
23. Kundie, F.; Azhari, C.H.; Muchtar, A.; Ahmad, Z.A. Effects of filler size on the mechanical properties of polymer-filled dental composites: A review of recent developments. *J. Phys. Sci.* **2018**, *29*, 141–165.
24. Gull, N.; Khan, S.M.; Munawar, M.A.; Shafiq, M.; Anjum, F.; Butt, M.T.Z.; Jamil, T. Synthesis and characterization of zinc oxide (ZnO) filled glass fiber reinforced polyester composites. *Mater. Des*. **2015**, *67*, 313–317. https://doi.org/10.1016/j.matdes.2014.11.021.
25. Najafi, A.; Golestani-Fard, F.; Rezaie, H.R.; Ehsani, N. Effect of APC addition on stability of nanosize precursors in sol–gel processing of SiC nanopowder. *J. Alloys Compd.* **2020**, *505*, 692–697. https://doi.org/10.1016/j.jallcom.2010.06.116.
26. Najafi, A.; Fard, F.G.; Rezaie, H.R.; Ehsani, N. Synthesis and characterization of SiC nano powder with low residual carbon processed by sol–gel method. *Powder Technol.* **2012**, *219*, 202–210. https://doi.org/10.1016/j.powtec.2011.12.045 10.1016/j.powtec.2011.12.045.
27. Kavecký, Š.; Janeková, B.; Madejová, J.; Šajgalík, P. Silicon carbide powder synthesis by chemical vapour deposition from silane/acetylene reaction system. *J. Eur. Ceram. Soc.* **2000**, *20*, 1939–1946. https://doi.org/10.1016/s0955-2219(00)00071-6.
28. Mas'udah, K.W.; Diantoro, M.; Fuad, A. Synthesis and Structural Analysis of Silicon Carbide from Silica Rice Husk and Activated Carbon Using Solid-State Reaction. *J. Phys. Conf. Ser.* **2018**, *1093*, 012033. https://doi.org/10.1088/1742-6596/1093/1/012033.
29. Singh, D.P.; Yadav, R.M.; Srivastava, O.N. Synthesis of Nanostructured Silicon Carbide Films Through Spray Pyrolysis of Ball-Milled Silicon. *Chem. Vap. Depos.* **2005**, *11*, 403–407. https://doi.org/10.1002/cvde.200504213.
30. Kalinina, E.V.; Lebedev, A.A.; Bogdanova, E.; Berenquier, B.; Ottaviani, L.; Violina, G.N.; Skuratov, V.A. Irradiation of 4H-SiC UV detectors with heavy ions. *Semiconductors* **2015**, *49*, 540–546. https://doi.org/10.1134/s1063782615040132.
31. Huczko, A.; Dąbrowska, A.; Savchyn, V.; Popov, A.I.; Karbovnyk, I. Silicon carbide nanowires: Synthesis and cathodoluminescence. *Phys. Status Solidi (B)* **2009**, *246*, 2806–2808. https://doi.org/10.1002/pssb.200982321.
32. Qian, M.; Xu, X.; Qin, Z.; Yan, S. Silicon carbide whiskers enhance mechanical and anti-wear properties of PA6 towards potential applications in aerospace and automobile fields. *Compos. Part B Eng.* **2019**, *175*, 107096. https://doi.org/10.1016/j.compositesb.2019.10.
33. Arpitha, G.R.; Sanjay, M.R.; Senthamaraikannan, P.; Barile, C.; Yogesha, B. Hybridization Effect of Sisal/Glass/Epoxy/Filler Based Woven Fabric Reinforced Composites. *Exp. Tech.* **2017**, *41*, 577–584. https://doi.org/10.1007/s40799-017-0203-4.
34. Mun, S.Y.; Lim, H.M.; Lee, D.-J. Thermal conductivity of a silicon carbide/pitch-based carbon fiber-epoxy composite. *Thermochim. Acta* **2015**, *619*, 16–19. https://doi.org/10.1016/j.tca.2015.09.020.
35. Suresha, B.; Chandramohan, G.; Renukappa, N.M.; Siddaramaiah. Influence of silicon carbide filler on mechanical and dielectric properties of glass fabric reinforced epoxy composites. *J. Appl. Polym. Sci.* **2008**, *111*, 685–691. https://doi.org/10.1002/app.29116.
36. Li, Y.; Chen, C.; Li, J.T.; Yang, Y.; Lin, Z.M. Surface charges and optical characteristic of colloidal cubic SiC nanocrystals. *Nanoscale Res. Lett*. **2011**, *6*, 454. Available online: http://www.nanoscalereslett.com/content/6/1/454 (accessed on 7 May 2022).
37. Hapuhinna, H.; Gunaratne, R.D.; Pitawala, H.M. Synthesis of bone cement from a natural mineral for biomedical industry. *Int. J. Sci. Res. Publ.* **2019**, *9*, p8872.
38. Hapuhinna, K.; Gunaratne, R.D.; Pitawala, J. A ceramic composite derived from high-grade rock phosphate as a substitution for human bone. *Mater. Technol.* **2019**, *34*, 743–750. https://doi.org/10.1080/10667857.2019.1623531.
39. Panda, R.N.; Hsieh, M.F.; Chung, R.J.; Chin, T.S. FTIR, XRD, SEM and solid state NMR investigations of carbonate-containing hydroxyapatite nano-particles synthesized by hydroxide-gel technique. *J. Phys. Chem. Solids* **2003**, *64*, 193–199.
40. Karbovnyk, I.; Savchyn, P.; Huczko, A.; Cestelli Guidi, M.; Mirri, C.; Popov, A.I. FTIR studies of silicon carbide 1D-nanostructures. In *Materials Science Forum*; Trans Tech Publications, Ltd.: Bäch, Switzerland, 2015; Volume 821, pp. 261–264.